

Data Efficient Prediction of Minimum Operating Voltage via Inter- and Intra-Wafer Variation Alignment

Yuxuan Yin

*Electrical and Computer Engineering
University of California
Santa Barbara, CA, USA
y_yin@ucsb.edu*

Rebecca Chen

*Automotive Processing
NXP Semiconductors
Austin, TX, USA
rebecca.chen_1@nxp.com*

Chen He

*Automotive Processing
NXP Semiconductors
Austin, TX, USA
chen.he@nxp.com*

Peng Li

*Electrical and Computer Engineering
University of California
Santa Barbara, CA, USA
lip@ucsb.edu*

Abstract—Predicting the minimum operating voltage (V_{min}) of chips stands as a crucial technique in enhancing the speed and reliability of manufacturing testing flow. However, existing V_{min} prediction methods often overlook various sources of variations in both training and deployment phases. Notably, the neglect of wafer zone-to-zone (intra-wafer) variations and wafer-to-wafer (inter-wafer) variations, compounded by process variations, diminishes the accuracy, data efficiency, and reliability of V_{min} predictors. To address this gap, we introduce a novel data-efficient V_{min} prediction flow, termed restricted bias alignment (RBA), which incorporates a novel variation alignment technique. Our approach concurrently estimates inter- and intra-wafer variations. Furthermore, we propose utilizing class probe data to model inter-wafer variations for the first time. We empirically demonstrate RBA’s effectiveness and data efficiency on an industrial 16nm automotive chip dataset.

Index Terms—chip performance prediction, machine learning, process variation, data alignment

I. INTRODUCTION

The measurement of the minimum operating voltage (V_{min}) represents a pivotal testing procedure crucial for assessing chip performance. It enables the identification of substandard products, facilitates power consumption optimization, and serves as an early indicator of potential failures during the device’s lifespan. A case study involving 7nm industry chips illustrates that subjecting all chips to uniform energy levels leads to a minimum 16% increase in energy utilization [1].

As technology nodes continue to shrink, the significance of V_{min} tests employing structural test patterns (e.g., SCAN) amplifies, becoming indispensable for pinpointing minute flaws and defects [2] within chips. For instance, in Fin Field-Effect Transistor (FinFET) technology, a resistive short defect within a critical path may augment leakage current, potentially evading detection through IDDQ testing due to high background leakage. However, such defects can manifest as discernible V_{min} degradation when subjected to V_{min} testing (e.g., SCAN V_{min}) traversing the affected critical path.

Testing V_{min} voltage incrementally for each die during manufacturing is impractical due to its time-consuming nature. Instead, a pragmatic approach involves testing V_{min} within a predefined target range, rather than exhaustively covering the

entire testing space. However, owing to process variations, chip properties exhibit variability from die to die, wafer zone to wafer zone, and wafer to wafer. The presence of such variations precludes the establishment of a fixed target V_{min} , as doing so would lead to significant underkill for failures and overkill for normal dies.

Current industrial practices rely on die-level features to construct V_{min} prediction models that account for die-to-die variations. These features, gathered from parametric tests or on-chip monitors such as IDDQ tests and ring oscillators [3], [4], serve as inputs to machine learning-based V_{min} predictors [5]–[9]. However, existing methodologies fall short in capturing wafer zone-to-zone (intra-wafer) and wafer-to-wafer (inter-wafer) variations. Fig. 1a and Fig. 1b illustrate the impact of inter- and intra-wafer variations to V_{min} and parametric features in an industrial 16nm chip dataset, respectively. It is evident that either type of process variation significantly alters the distribution of V_{min} and parametric features, ultimately impairing the accuracy of aforementioned V_{min} predictors.

In this paper, we introduce a novel V_{min} prediction framework called restricted bias alignment (RBA), designed to systematically capture inter- and intra-wafer variations, along with die-to-die variations. To address die-level variations, we adopt parametric test features in line with prior research. However, for inter- and intra-wafer variations, we treat them as independent and employ a voltage bias term to model their respective impacts on individual dies. Additionally, we harness class probe data to model inter-wafer variations. By aligning and modeling process variations, RBA is data-efficient and robust when training, and is accurate in deployment for dies from new wafers. Our main contributions are:

- We propose a novel data-efficient algorithm for estimating and aligning V_{min} shifts resulting from inter- and intra-wafer variations.
- We propose to utilize class probe data for inter-wafer V_{min} shift modeling for the first time, and propose to reuse pre-learned intra-wafer V_{min} shift for dies from new wafers in addressing process variations.
- Through empirical analysis, we demonstrate the effec-

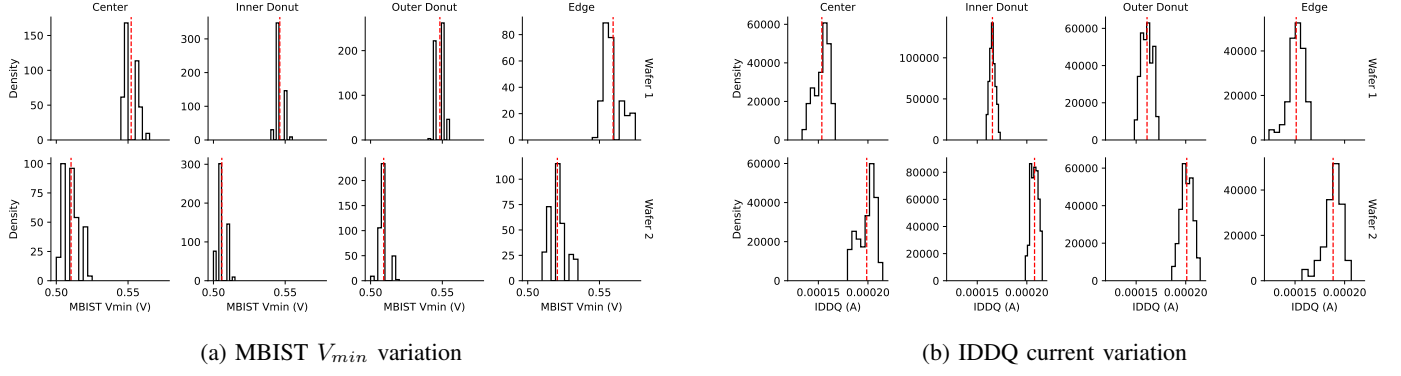


Figure 1: Wafer-to-wafer and wafer zone variations across 2 wafers, measured at 25°C. Red dashed lines represent mean values.

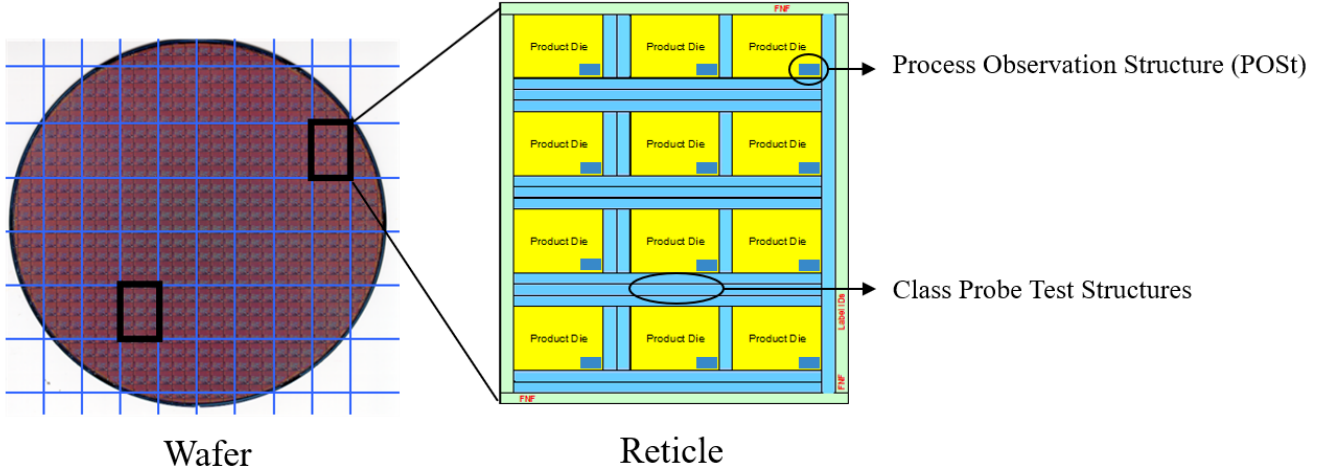


Figure 2: Class probe test structures and process observation structures

tiveness and data efficiency of the proposed V_{min} prediction approach on an industrial dataset.

II. PRELIMINARIES

A. Testing Flow in Semiconductor Manufacturing

In semiconductor manufacturing, wafer-level testing employs class probe test structures that are situated in the scribe lines between product dies, outside the actual chips, as depicted in Fig. 2. These test structures typically contain components like transistors, via chains, resistors, and capacitors, mirroring the fabrication process used for the product dies. The purpose of these test structures is to provide feedback on the wafer’s processing, enable statistical process control, and help reduce variations from wafer to wafer.

At the die level, each part incorporates its own set of test structures, known as Process Observation Structures (POSt), typically located at the corners of each die. These structures include components like ring oscillators, transistors, bipolar junctions, resistors, and capacitors, which reflect the elements used in the actual circuits on each die. POSt structures offer visibility into the die-level processing, allowing engineers to monitor and evaluate the performance of individual dies. Fig. 3

shows an example of a highly parallel probe hardware system. The probe card touches down on multiple Devices Under Test (DUTs) on the wafer to drive electrical stimulus to all dies being tested. Following a predefined algorithm, the probe card moves around to cover the entire wafers.

Together, these two sets of test structures—the class probe at the wafer level and the POSt at the die level—create a hierarchical system for tracking process variations across wafers and individual dies. This setup allows for correlations between class probe data and inter-wafer V_{min} bias, as well as between POSt data and the V_{min} of individual dies. The presence of these correlations indicates that the test structures can be used to predict and control process variations, contributing to more reliable and consistent chip production.

B. Linear Regression for V_{min} Prediction

Linear regression is a simple yet effective method to predict V_{min} . It builds upon the following assumption

$$y = \mathbf{x}\mathbf{w} + b + \epsilon \quad (1)$$

where $y \in (0, +\infty)$ is the positive value of V_{min} , $\mathbf{x} \in \mathbb{R}^{1 \times d}$ is a d -dimensional row vector, which is a subset of features

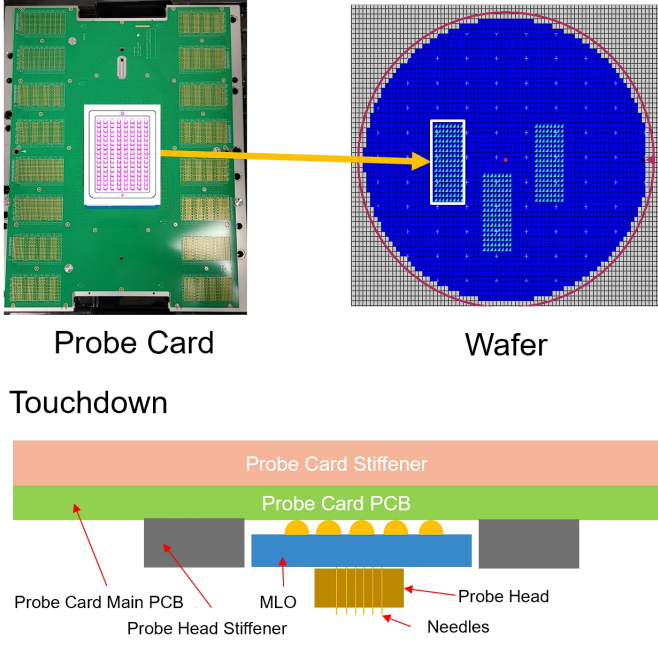


Figure 3: A highly-parallel wafer probe touchdown

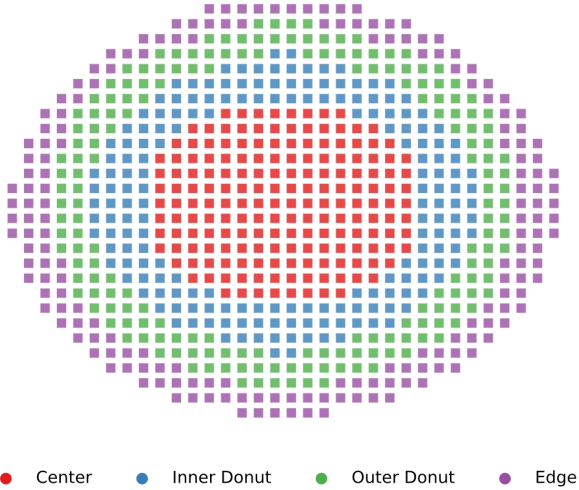


Figure 4: A balanced wafer region partition into 4 regions

measured by parametric tests, $\mathbf{w} \in \mathbb{R}^{d \times 1}$ is a d -dimensional column vector of unknown parameters, $b \in \mathbb{R}$ is a bias term of V_{min} , and $\epsilon \in \mathbb{R}$ accounts for the influence on V_{min} other than features \mathbf{x} .

Given a training dataset (\mathbf{X}, \mathbf{y}) , one can estimate $\hat{\mathbf{w}}$ and \hat{b} via minimizing the sum of square residuals

$$\hat{\mathbf{w}}, \hat{b} = \arg \min_{\mathbf{w}, b} \|\mathbf{y} - \mathbf{X}\mathbf{w} - b\|_2^2 \quad (2)$$

and the solution is

$$\hat{\mathbf{w}} = (\tilde{\mathbf{X}}^T \tilde{\mathbf{X}})^{-1} \tilde{\mathbf{X}}^T \tilde{\mathbf{y}} \quad (3)$$

$$\hat{b} = \bar{\mathbf{y}} - \bar{\mathbf{X}} \hat{\mathbf{w}} \quad (4)$$

where the bar operator $\bar{\cdot}$ computes the mean value (vector) of a vector (matrix), and the tilde operator $\tilde{\cdot}$ centralizes the input.

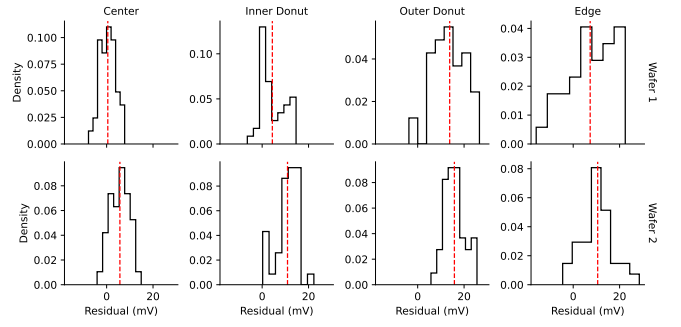


Figure 5: Variation of testing residuals of V_{min} prediction of a linear regression trained on dies from the center zone from wafer 1. Red dashed lines represent mean values.

The learned parameters $\hat{\mathbf{w}}$ and \hat{b} are used to predict V_{min} of new dies. For a new chip, we perform parametric tests to collect the input feature \mathbf{x}^{test} for linear regression, and then compute the V_{min} prediction \hat{y}^{test} :

$$\hat{y}^{test} = \mathbf{x}^{test} \hat{\mathbf{w}} + \hat{b} \quad (5)$$

C. Influence of Inter- and Intra-Wafer Variation on V_{min} Prediction

Process variations are inherent in modern semiconductor manufacturing, with their significance magnifying as technology nodes and wafer sizes scale. Typically, there are two types of process variations: inter-wafer (wafer-to-wafer) variations and intra-wafer (zone-to-zone) variations.

We visually depict the contributions of both variations to the distribution of V_{min} and parametric features within our industrial 16nm automotive dataset in Fig. 1. Specifically, we present histogram plots and mean values of MBIST V_{min} in Fig. 1a and IDDQ current in Fig. 1b, spanning the four regions of two wafers from the same lot. Each row in either sub-figure represents the intra-wafer variation of a given wafer, while each column signifies the inter-wafer variations of a specific wafer zone.

It is evident that both V_{min} and parametric feature distributions exhibit considerable variance across wafers and regions. However, if process variations merely introduce *covariate shift*, wherein the relationship $y|x$ between V_{min} and parametric features remains constant, we could feasibly train a V_{min} predictor and deploy it on new testing dies. Unfortunately, the assumption of covariate shift does not hold for the V_{min} prediction task. To illustrate, we train the aforementioned linear model on dies from the center zone of wafer 1 and test it across all four zones of wafers 1 and 2. The resulting residual of MBIST V_{min} on the testing data is depicted in Fig. 5, where the residual r is computed as

$$r = y - \hat{y} \quad (6)$$

The predictor performs admirably on the center zone of wafer 1; however, its accuracy notably declines on other testing wafer zones of both wafer 1 and wafer 2. This outcome underscores that process variations alter the statistical correlation between

V_{min} and parametric test features, rather than solely inducing covariate shift. Consequently, there arises a necessity to systematically address process variations, encompassing both inter- and intra-wafer variations, to attain accurate and robust V_{min} prediction.

III. DATA EFFICIENT INTER- AND INTRA-WAFER VARIATION ALIGNMENT

It is clear that both V_{min} and parametric features exhibit significant variation from wafer to wafer and from region to region. In this paper, we concentrate on a specific impact of process variations on the dependency $y|x$ between V_{min} and parameter features: a consistent voltage shift of V_{min} relative to the bias b .

We introduce two methods to align the V_{min} shift resulting from process variations. The first one, named Bias Alignment (BA), is a general machine learning method: it aims to estimate the voltage shift term of each wafer zone. The second method, known as Restricted Bias Alignment (RBA), is guided by domain knowledge: it assumes independence between inter- and intra-wafer variations, while the intra-wafer variation remains constant across all wafers. Additionally, for RBA, we propose utilizing class probe features to correlate the estimated inter-wafer V_{min} shift. This technique empowers RBA to predict V_{min} for dies from a new wafer without necessitating access to any training data from that wafer.

A. Bias Alignment (BA) for V_{min} Prediction

1) *Problem Formulation:* Assume we have N wafers in the training dataset. Each wafer is partitioned into M balanced wafer zones. We denote $(\mathbf{X}_{i,j}, \mathbf{y}_{i,j})$ as the collected (feature, V_{min}) pair of a batch of dies from the j -th zone of the i -th wafer. Here $i = 1, \dots, N$ and $j = 1, \dots, M$. Taking process variations into consideration, the V_{min} is modeled as

$$\mathbf{y}_{i,j} = \mathbf{X}_{i,j} \mathbf{w} + b_{i,j} + \epsilon \quad (7)$$

where \mathbf{w} is the fixed coefficients across wafer zones, and $b_{i,j}$ is a bias term of the i -th wafer's j -th zone, accounting for the impact of both inter- and intra-wafer variations.

We construct a loss function \mathcal{L}_{BA} as the sum of square residuals of the V_{min} prediction across the whole training set:

$$\mathcal{L}_{BA} := \sum_{i,j} \|\mathbf{y}_{i,j} - \mathbf{X}_{i,j} \mathbf{w} - b_{i,j}\|_2^2 \quad (8)$$

and minimize it to estimate $\hat{\mathbf{w}}$ and $\hat{\mathbf{b}}$

$$\hat{\mathbf{w}}, \hat{\mathbf{b}} = \arg \min_{\mathbf{w}, \mathbf{b}} \mathcal{L}_{BA}(\mathbf{w}, \mathbf{b}) \quad (9)$$

where \mathbf{b} is a set containing all biases $b_{i,j}$.

2) *Solution:* We provide analytical solution of Eq. (9). For $\hat{\mathbf{w}}$ and $\hat{\mathbf{b}}$ we should have

$$\frac{\partial \mathcal{L}_{BA}}{\partial \hat{\mathbf{w}}} = 0 \quad (10)$$

$$\frac{\partial \mathcal{L}_{BA}}{\partial \hat{\mathbf{b}}} = 0 \quad (11)$$

Zone	Center	Inner Donut	Outer Donut	Edge
# Dies	180	184	184	183

Table I: The number of dies in each wafer zone

From Eq. (13) we have

$$\frac{\partial}{\partial \hat{b}_{i,j}} \|\mathbf{y}_{i,j} - \mathbf{X}_{i,j} \hat{\mathbf{w}} - \hat{b}_{i,j}\|_2^2 = 0 \quad (12)$$

which means that

$$\hat{b}_{i,j} = \bar{\mathbf{y}}_{i,j} - \bar{\mathbf{X}}_{i,j} \hat{\mathbf{w}} \quad (13)$$

Then Eq. (15) can be formulated as

$$\frac{\partial}{\partial \hat{\mathbf{w}}} \sum_{i,j} \|\bar{\mathbf{y}}_{i,j} - \bar{\mathbf{X}}_{i,j} \hat{\mathbf{w}}\|_2^2 = 0 \quad (14)$$

where we can directly compute the formula of $\hat{\mathbf{w}}$:

$$\hat{\mathbf{w}} = \left(\sum_{i,j} \tilde{\mathbf{X}}_{i,j}^T \tilde{\mathbf{X}}_{i,j} \right)^{-1} \left(\sum_{i,j} \tilde{\mathbf{X}}_{i,j}^T \tilde{\mathbf{y}}_{i,j} \right) \quad (15)$$

3) *Discussion:* The estimated coefficient $\hat{\mathbf{w}}$ and bias $\hat{\mathbf{b}}$ in BA aggregate the information from dies of all wafer zones, and meanwhile tackle individual V_{min} shift of each wafer zone caused by inter- and intra-wafer variations. Compared with the vanilla linear regression presented in Section II-B, BA is more data-efficient and accurate for V_{min} prediction.

For a testing die $(\mathbf{x}_{i,j}^{test}, y_{i,j}^{test})$ from the j -th zone of the i -th wafer, the V_{min} prediction of BA is

$$\hat{y}^{test} = \mathbf{x}^{test} \hat{\mathbf{w}} + \hat{b}_{i,j} \quad (16)$$

However, in the V_{min} inference process, BA necessitates the computation of the voltage shift term in advance. Consequently, testing V_{min} for several dies from a new wafer (wafer zone) remains necessary. This inherent limitation inspires our second V_{min} prediction approach, wherein no V_{min} test is required for the new wafer (wafer zone).

B. Restricted Bias Alignment (RBA) for V_{min} Prediction

RBA operates under the assumption that intra-wafer and inter-wafer variations are independent. This assumption is motivated by observations from Fig. 1, where the intra-wafer variation appears consistent across wafers, while the inter-wafer variation remains stable across wafer regions.

Moreover, RBA introduces the use of class probe features to model inter-wafer variations. By leveraging the pre-learned intra-wafer variations and the predicted inter-wafer variations, RBA demonstrates the capability to predict V_{min} for a die from a new wafer without necessitating further data collection.

1) *Problem Formulation:* Denote $\mathbf{z}_i \in \mathbb{R}^k$ as the vector of k class probe features of the i -th wafer, RBA models V_{min} as

$$\mathbf{y}_{i,j} = \mathbf{X}_{i,j} \mathbf{w} + b_i(\mathbf{z}_i) + b_j^{intra} + \epsilon \quad (17)$$

where b_j^{intra} accounts for the V_{min} shift caused by intra-wafer variations; $b_i^{inter}(\mathbf{z}_i)$ is a linear model of \mathbf{z}_i , representing the voltage bias of wafer i :

$$b_i^{inter} = \mathbf{z}_i \mathbf{w}_z + b_z + \epsilon_z \quad (18)$$

Table II: The testing RMSE (mV) of DC Scan V_{min} prediction with 75% data for training

Temperature		-45°C				25°C			
Wafer ID	Wafer Zone	# Die	Linear Regression	Bias Alignment	Restricted BA	# Die	Linear Regression	Bias Alignment	Restricted BA
1	Center	166	3.54	2.69	2.88	165	3.28	2.72	2.68
1	Inner Donut	162	5.35	3.71	4.14	161	5.03	4.12	4.64
1	Outer Donut	158	7.69	3.24	3.28	173	4.79	3.92	3.91
1	Edge	91	5.21	3.34	3.05	128	5.17	4.82	4.78
2	Center	152	11.84	3.80	4.90	166	6.13	3.63	3.98
2	Inner Donut	153	8.23	3.57	3.85	172	5.16	3.62	3.79
2	Outer Donut	155	5.04	3.25	3.59	172	4.37	4.03	3.89
2	Edge	93	9.39	5.60	5.58	128	7.82	5.51	5.72
3	Center	54	8.03	4.46	4.37	152	5.49	4.36	4.38
3	Inner Donut	111	5.19	3.05	3.49	168	3.98	3.06	3.46
3	Outer Donut	126	5.74	4.52	4.69	173	4.50	4.43	4.72
3	Edge	89	4.03	4.07	4.27	130	4.66	4.68	4.71
4	Center	138	4.25	3.73	3.60	161	3.58	2.43	2.38
4	Inner Donut	157	3.98	2.72	2.72	174	3.63	3.32	3.46
4	Outer Donut	154	5.16	2.92	2.94	171	5.61	3.93	3.88
4	Edge	91	3.52	3.56	3.55	128	5.18	4.58	4.88
5	Center	153	5.98	3.12	3.49	171	3.80	2.70	3.02
5	Inner Donut	158	4.34	3.12	3.11	172	4.23	3.14	3.43
5	Outer Donut	160	6.11	3.40	3.44	178	6.15	5.36	5.28
5	Edge	104	4.40	4.27	4.32	141	4.23	4.25	4.25
Mean		-	6.20	3.56	<u>3.75</u>	-	4.91	3.97	<u>4.10</u>

Table III: The testing RMSE (mV) of AC Scan V_{min} prediction with 75% data for training

Temperature		-45°C				25°C			
Wafer ID	Wafer Zone	# Die	Linear Regression	Bias Alignment	Restricted BA	# Die	Linear Regression	Bias Alignment	Restricted BA
1	Center	166	7.71	5.08	5.01	164	5.49	4.72	4.62
1	Inner Donut	162	6.70	6.33	6.49	159	6.54	6.12	6.20
1	Outer Donut	158	5.29	5.53	5.45	173	8.90	5.79	5.63
1	Edge	90	6.66	5.85	6.19	123	9.43	8.32	8.44
2	Center	152	12.06	5.57	6.00	165	13.69	5.17	6.10
2	Inner Donut	153	7.35	6.77	6.83	170	7.23	6.23	5.81
2	Outer Donut	155	6.10	6.34	6.58	170	6.16	6.29	6.41
2	Edge	93	5.27	4.61	4.48	121	7.66	6.19	5.88
3	Center	54	11.52	6.84	7.22	151	7.94	5.88	6.37
3	Inner Donut	110	8.72	5.82	6.23	165	7.77	6.03	6.25
3	Outer Donut	126	7.82	6.30	6.59	172	6.88	6.78	6.95
3	Edge	89	8.98	8.43	8.84	127	7.24	7.83	8.52
4	Center	138	6.48	4.67	5.10	160	5.78	5.64	5.96
4	Inner Donut	157	9.33	6.59	6.72	172	6.09	4.96	5.48
4	Outer Donut	154	12.21	7.18	7.30	168	11.23	7.29	7.38
4	Edge	91	10.59	6.52	6.65	123	9.07	8.15	8.34
5	Center	153	5.54	5.38	5.01	172	6.53	6.18	6.17
5	Inner Donut	158	6.09	6.31	6.24	170	5.86	5.66	5.78
5	Outer Donut	159	6.95	6.56	6.83	176	9.29	6.22	6.19
5	Edge	103	6.39	6.44	6.89	136	7.30	6.87	6.20
mean	-	-	8.05	6.17	<u>6.33</u>	-	8.04	6.31	<u>6.43</u>

We construct a loss function \mathcal{L}_{RBA} as the sum of square residuals of the V_{min} prediction across the whole training set:

$$\mathcal{L}_{RBA} := \sum_{i,j} \|\mathbf{y}_{i,j} - \mathbf{X}_{i,j} \mathbf{w} - \mathbf{b}_i^{inter} - \mathbf{b}_j^{intra}\|_2^2 \quad (19)$$

where \mathbf{b} is a set of V_{min} shift of inter- and intra-wafer variations. We minimize the loss function it to estimate \mathbf{w} ,

\mathbf{b}^{inter} , and \mathbf{b}^{intra} :

$$\hat{\mathbf{w}}, \hat{\mathbf{b}}^{inter}, \hat{\mathbf{b}}^{intra} = \arg \min_{\mathbf{w}, \mathbf{b}^{inter}, \mathbf{b}^{intra}} \mathcal{L}_{RBA}(\mathbf{w}, \mathbf{b}^{inter}, \mathbf{b}^{intra}) \quad (20)$$

2) *Solution:* To directly solve Eq. (20) is complicated. We adopt an alternative one-step gradient descent approach, integrating a novel initialization method to accelerate the convergence. Denote $\mathbf{w}_{(t)}$, $\mathbf{b}_{(t)}^{inter}$, and $\mathbf{b}_{(t)}^{intra}$ as the estimated parameters in the training step t .

In step 0, we utilize BA to initialize parameters: $\mathbf{w}_{(0)}$ takes

Table IV: The testing RMSE (mV) of MBST V_{min} prediction with 75% data for training

Temperature		-45°C				25°C			
Wafer ID	Wafer Zone	# Die	Linear Regression	Bias Alignment	Restricted BA	# Die	Linear Regression	Bias Alignment	Restricted BA
1	Center	166	8.73	2.58	2.64	165	4.54	2.85	3.40
1	Inner Donut	162	9.91	3.25	3.37	161	8.97	3.53	4.18
1	Outer Donut	158	9.34	4.76	4.72	173	10.10	4.49	4.45
1	Edge	90	13.10	9.76	11.94	120	15.98	9.77	11.17
2	Center	135	6.46	3.69	4.04	166	11.05	3.43	3.49
2	Inner Donut	136	5.19	3.70	3.69	172	8.07	2.68	2.71
2	Outer Donut	80	5.48	3.92	3.50	172	5.62	3.74	3.71
2	Edge	59	10.54	4.83	4.85	124	13.17	7.29	7.08
3	Center	54	8.99	3.35	3.52	152	8.24	4.20	4.10
3	Inner Donut	111	5.54	3.27	3.29	165	5.54	2.66	2.62
3	Outer Donut	125	5.67	3.04	3.05	174	6.70	2.56	2.56
3	Edge	88	9.05	6.69	6.69	123	11.83	7.32	7.34
4	Center	138	30.50	4.23	6.24	161	24.39	4.22	5.68
4	Inner Donut	157	24.24	3.20	3.13	174	14.82	3.08	3.21
4	Outer Donut	153	22.69	3.46	4.35	171	10.59	3.01	3.04
4	Edge	91	28.54	5.12	6.96	128	13.90	5.28	6.32
5	Center	153	19.38	4.62	4.65	172	18.45	4.64	4.89
5	Inner Donut	158	18.20	4.44	4.51	172	24.10	4.31	4.34
5	Outer Donut	159	19.46	4.30	4.42	178	25.02	4.24	4.42
5	Edge	104	13.10	5.80	5.78	138	19.39	6.69	6.77
mean	-	-	16.25	4.45	<u>4.91</u>	-	14.47	4.63	<u>4.94</u>

the value of the right-hand side of Eq. (15); $\mathbf{b}_{(0)}^{inter}$, and $\mathbf{b}_{(0)}^{intra}$ are the mean vector of the right-hand side of Eq. (13) by column and row, respectively.

In step t , we first optimize $\mathbf{w}_{(t)}$ to minimize \mathcal{L}_{RBA} , condition on $\mathbf{b}_{(t-1)}^{inter}$ and $\mathbf{b}_{(t-1)}^{intra}$:

$$\mathbf{w}_{(t)} = \arg \min_{\mathbf{w}} \mathcal{L}_{RBA}(\mathbf{w}, \mathbf{b}_{(t-1)}^{inter}, \mathbf{b}_{(t-1)}^{intra}) \quad (21)$$

This is a linear regression problem and the solution is

$$\mathbf{w}_{(t)} = (\mathbf{X}^T \mathbf{X})^{-1} \mathbf{X}^T \mathbf{y}_{(t)} \quad (22)$$

where $(\mathbf{X}, \mathbf{y}_{(t)})$ is the concatenation of data of all wafer zones $(\mathbf{X}_{i,j}, \mathbf{y}_{i,j} - \mathbf{b}_{i;(t-1)}^{inter} - \mathbf{b}_{j;(t-1)}^{intra})$.

Then, we adopt the chain rule to update biases:

$$\mathbf{b}_{(t)}^{inter} = \mathbf{b}_{(t-1)}^{inter} - \eta \left(\frac{\partial \mathcal{L}_{RBA}}{\partial \mathbf{w}_{(t)}} \cdot \frac{\partial \mathbf{w}_{(t)}}{\partial \mathbf{b}_{(t-1)}^{inter}} \right)^T \quad (23)$$

$$\mathbf{b}_{(t)}^{intra} = \mathbf{b}_{(t-1)}^{intra} - \eta \left(\frac{\partial \mathcal{L}_{RBA}}{\partial \mathbf{w}_{(t)}} \cdot \frac{\partial \mathbf{w}_{(t)}}{\partial \mathbf{b}_{(t-1)}^{intra}} \right)^T \quad (24)$$

where η is a hyper-parameter of learning rate.

Once the training process is done, we optimize the coefficients of class probe features:

$$\hat{\mathbf{w}}_{\mathbf{z}}, \hat{\mathbf{b}}_{\mathbf{z}} = \arg \min_{\mathbf{w}_{\mathbf{z}}, \mathbf{b}_{\mathbf{z}}} \sum_i \|\hat{\mathbf{b}}_i^{inter} - \mathbf{z}_i \mathbf{w}_{\mathbf{z}} - \mathbf{b}_{\mathbf{z}}\|_2^2 \quad (25)$$

3) *Discussion*: RBA effectively separates the influence of inter- and intra-wafer variations on V_{min} shift. This decoupling mechanism distinguishes RBA from BA, mitigating potential overfitting concerns particularly when dealing with small training datasets, thereby bolstering overall data efficiency.

For a testing die $(\mathbf{x}_{i,j}^{test}, \mathbf{y}_{i,j}^{test})$ form the j -th zone of the i -th wafer, the V_{min} prediction of RBA is

$$\hat{\mathbf{y}}^{test} = \mathbf{x}^{test} \hat{\mathbf{w}} + \hat{\mathbf{b}}_i^{inter}(\mathbf{z}_i) + \hat{\mathbf{b}}_j^{intra} \quad (26)$$

where

$$\hat{\mathbf{b}}_i^{inter}(\mathbf{z}_i) = \mathbf{z}_i \mathbf{w}_{\mathbf{z}} + \mathbf{b}_{\mathbf{z}} \quad (27)$$

By incorporating class probe features to capture inter-wafer variations, RBA possesses the capability for deployment in V_{min} prediction without necessitating re-training or measuring V_{min} for any dies from a new wafer. This feature enhances the practical applicability and efficiency of RBA in product testing scenarios.

IV. EXPERIMENTAL RESULTS

We conduct experiments to demonstrate the efficacy of our approach RBA for addressing inter- and intra-wafer variations on thousands of 16nm automotive chips. We aim to illustrate: 1) the effectiveness of V_{min} bias alignment, 2) the data efficiency and robustness of RBA, 3) the capability of class probe features to capture inter-wafer variation, and 4) the ability of RBA to predict V_{min} of dies from a new wafer.

a) *Description of Data Collection*: We get the class probe data of each wafer from the foundry. During the testing flow of product manufacturing, V_{min} , including DC Scan V_{min} , AC Scan V_{min} , and MBIST V_{min} are measured at at three different temperatures: -45°C (cold), 25°C (room), and 125°C (hot). Similarly, parametric test and POST test data were collected under different temperatures from Automatic Test Equipment (ATE) testers.

Our dataset has several wafers. Each wafer is partitioned into 4 zones: center, inner donut, outer donut, and edge. The visualization of this partition is shown in Fig. 4, and the number

Table V: Inter-wafer V_{min} shift (mV) from wafer 1 estimated by RBA

Wafer ID	Temp.	DC Scan V_{min}	AC Scan V_{min}	MBST V_{min}
2	-45°C	-18.78	-6.93	-14.41
3	-45°C	-4.32	-4.45	-6.87
4	-45°C	-5.98	5.69	-28.93
5	-45°C	-3.28	2.35	17.68
2	25°C	-9.91	-10.03	-18.75
3	25°C	2.18	-4.10	-8.77
4	25°C	0.62	6.60	-27.99
5	25°C	-0.37	7.48	-18.02

Table VI: Intra-wafer V_{min} shift (mV) from center zone estimated by RBA

Wafer Zone	Temp.	DC Scan V_{min}	AC Scan V_{min}	MBST V_{min}
Inner Donut	-45°C	2.48	4.16	7.35
Outer Donut	-45°C	2.87	6.81	-2.17
Edge	-45°C	1.36	5.65	-1.18
Inner Donut	25°C	2.32	4.22	-1.03
Outer Donut	25°C	3.13	6.95	-2.24
Edge	25°C	-0.35	3.47	-11.15

of dies in each wafer zone is listed in Table I. Due to the expensive cost of V_{min} test, only a subset of dies is performed the V_{min} test for a certain test pattern.

b) RBA Settings: RBA leverages 5 parametric test features and 2 class probe features as input to predict V_{min} . All features are selected by the Correlation Feature Selection algorithm [10], and pass the causation check by our testing engineer. The hyper-parameter learning rate η is set to 0.1. We terminate the training process when the relative improvement of the loss function \mathcal{L}_{RBA} is smaller than 0.001.

c) Baseline Settings: We compare RBA with 2 baselines: linear regression, and the proposed Bias Alignment (BA). Linear regression is trained over all of the label data without handling process variations. To ensure a fair comparison, all the baselines and RBA share the same general configurations, including input features, training data, and testing data.

A. Effectiveness of V_{min} bias alignment

We aim to showcase the effectiveness of V_{min} bias alignment in the V_{min} prediction task.

a) Experimental Settings: We consider all three types of V_{min} (DC Scan, AC Scan, and MBST), tested at cold and room temperatures. Our dataset comprises 5 wafers tested under these conditions. For each wafer zone, we allocate 75% of the dies for training and the remaining 25% for testing. The methods under consideration include linear regression, BA, and RBA.

b) Results: We report the testing RMSE of V_{min} prediction in each wafer zone, and the average result across the whole testing dataset in Table II for DC Scan V_{min} , Table III for AC Scan V_{min} , and Table IV for MBST V_{min} . The bold number represents the best method, and the underlined number represents the second-best method. In each V_{min} prediction task, both BA and RBA consistently outperform the baseline linear regression. This suggests that the bias alignment

Table VII: RBA with different fractions of data for training

Temperature Training data frac.	-45°C		25°C	
	75%	5%	75%	5%
DC Scan V_{min} (mV)	3.75	3.85	4.10	3.82
AC Scan V_{min} (mV)	6.33	6.42	6.43	6.54
MBST V_{min} (mV)	4.91	5.03	4.94	5.18

Table VIII: Top 1 linear correlation between class probe features and inter-wafer V_{min} shift estimated by RBA

Test Pattern	DC Scan V_{min}	AC Scan V_{min}	MBST V_{min}
Top 1 Linear Corr.	0.892	0.948	0.953

technique effectively captures process variations. Notably, the performance gap between BA and RBA is minimal, indicating a weak dependency between inter- and intra-wafer variations.

Additionally, we show the inter- and intra-wafer V_{min} shift estimated by our approach RBA in Table V and Table VI, respectively. The variance of both types of V_{min} shift is substantial and cannot be disregarded. A significant V_{min} shift notably impacts the accuracy of linear regression. For instance, linear regression performs badly for predicting DC Scan V_{min} of wafer 2 at the cold temperature, where a -18.78mV V_{min} shift is estimated by RBA.

B. Data Efficiency and Robustness of RBA

We present the performance of RBA on small training datasets to demonstrate its data efficiency and robustness.

a) Experimental Settings: We split 5% dies in each wafer zone for training, and the rest for testing. All other configurations are the same as those in Section IV-A.

b) Results: The V_{min} prediction accuracy of RBA is listed in Table VII. While the fraction of training data is reduced from 75% to 5% (around 7 dies in each wafer zone), RBA's accuracy is stable, indicating its superior data efficiency and robustness.

C. Class Probe Features Capturing Inter-Wafer Variation

We demonstrate that the dependency between class probe features and inter-wafer variations estimated by RBA is really high, indicating the motivation to leverage wafer-level class probe features to model wafer-to-wafer variation is plausible.

a) Experimental Settings: Our dataset has 10 wafers whose DC Scan, AC Scan, and MBST V_{min} are tested at the hot temperature. In the first step, we employ RBA on these wafers to collect 9 V_{min} shift terms relative to a base wafer. Subsequently, we correlate these shifts with each class probe feature, reporting the highest absolute value of the Pearson correlation coefficient. A higher coefficient indicates a stronger linear correlation. In the second step, we utilize the V_{min} shifts

Table IX: Coefficient of determination of the linear model using 2 class probe features to predict V_{min} shift estimated by RBA

Test Pattern	DC Scan V_{min}	AC Scan V_{min}	MBST V_{min}
R^2	0.509	0.631	0.792

Table X: The testing RMSE (mV) of V_{min} tested at 125°C

Method	DC Scan V_{min}	AC Scan V_{min}	MBST V_{min}
Linear Regression	7.33	9.40	14.24
RBA	8.07	8.98	9.18

of 6 wafers to fit a linear model for 2 class probe features and evaluate its testing coefficient of determination (R^2) on the remaining 4 wafers.

b) Results: In Table VIII, it is evident that for each V_{min} test pattern, there exists a class probe feature with a correlation coefficient of at least 0.89, indicating (1) the credibility of the inter-wafer V_{min} shift estimated by RBA, and (2) the informativeness of class probe data in modeling V_{min} shift across wafers.

Table IX reports the test accuracy of using class probe features to model V_{min} shift. The R^2 score of each V_{min} test pattern is proportion to the Pearson score in Table VIII. While MBST V_{min} shift predictors appear promising, we encounter difficulty in obtaining a sufficiently accurate predictor for the DC/AC Scan V_{min} shift. This challenge may stem from the small size of the training dataset, leading to an increased variance. We defer this issue to future research endeavors where a larger pool of tested wafers can be obtained.

D. RBA for V_{min} Prediction of New Wafer

We assess the effectiveness of RBA in predicting V_{min} of new wafers, focusing on addressing inter- and intra-wafer variations.

a) Experimental Settings: We evaluate RBA on the V_{min} prediction task, where V_{min} is tested at 125°C. Following Section IV-C, we use 6 wafers for training and 4 wafers for testing. The baseline model is linear regression.

b) Results: Table X presents the RMSE of RBA and linear regression. Owing to the limited number of wafers available in our dataset for training the inter-wafer V_{min} shift predictor, RBA and linear regression yield comparable results for DC/AC Scan V_{min} prediction. However, RBA exhibits a significant performance advantage over linear regression in the MBST V_{min} prediction task, highlighting its efficacy in addressing inter- and intra-wafer variations.

V. CONCLUSION

This paper introduces restricted bias alignment (RBA), a V_{min} prediction framework designed to systematically capture process variations in semiconductor manufacturing. By leveraging class probe features to model inter-wafer variations and utilizing parametric features to estimate intra-wafer variations, RBA offers a comprehensive approach to address the challenges posed by process variations.

Our experiments conducted on an industrial dataset demonstrate the effectiveness of RBA in mitigating the impact of process variations on V_{min} prediction. The results highlight the practical utility and robustness of RBA in real-world semiconductor manufacturing scenarios, underscoring its potential to enhance manufacturing efficiency and reliability.

ACKNOWLEDGMENT

The content of this paper has been developed with the support of Grant No. 1956313 from the National Science Foundation (NSF) and has also received partial funding from a Long Term University (LTU) grant provided by NXP.

REFERENCES

- [1] W.-C. Lin, C. Chen, C.-H. Hsieh, J. C.-M. Li, E. J.-W. Fang, and S. S.-Y. Hsueh, "MI-assisted vminbinning with multiple guard bands for low power consumption," in *2022 IEEE International Test Conference (ITC)*, 2022, pp. 213–218.
- [2] C. He and Y. Yu, "Wafer level stress: Enabling zero defect quality for automotive microcontrollers without package burn-in," in *2020 IEEE International Test Conference (ITC)*, 2020, pp. 1–10.
- [3] J. Keane, W. Zhang, and C. H. Kim, "An array-based odometer system for statistically significant circuit aging characterization," *IEEE Journal of Solid-State Circuits*, vol. 46, no. 10, pp. 2374–2385, 2011.
- [4] T.-B. Chan, P. Gupta, A. B. Kahng, and L. Lai, "Ddro: A novel performance monitoring methodology based on design-dependent ring oscillators," in *Thirteenth International Symposium on Quality Electronic Design (ISQED)*, 2012, pp. 633–640.
- [5] Y.-T. Kuo, W.-C. Lin, C. Chen, C.-H. Hsieh, J. C.-M. Li, E. Jia-Wei Fang, and S. S.-Y. Hsueh, "Minimum operating voltage prediction in production test using accumulative learning," in *2021 IEEE International Test Conference (ITC)*, 2021, pp. 47–52.
- [6] Q. Shi, X. Wang, L. Winemberg, and M. M. Tehranipoor, "On-chip sensor selection for effective speed-binning," *Analog Integrated Circuits and Signal Processing*, vol. 88, pp. 369–382, 2016.
- [7] J. Chen, J. Zeng, L.-C. Wang, M. Mateja, and J. Rearick, "Predicting multi-core system fmax by data-learning methodology," in *Proceedings of 2010 International Symposium on VLSI Design, Automation and Test*, 2010, pp. 220–223.
- [8] W.-C. Lin, C. Chen, C.-H. Hsieh, J. C.-M. Li, E. J.-W. Fang, and S. S.-Y. Hsueh, "MI-assisted vminbinning with multiple guard bands for low power consumption," in *2022 IEEE International Test Conference (ITC)*, 2022, pp. 213–218.
- [9] Y. Yin, R. Chen, C. He, and P. Li, "Domain-specific machine learning based minimum operating voltage prediction using on-chip monitor data," in *2023 IEEE International Test Conference (ITC)*, 2023, pp. 99–104.
- [10] M. A. Hall, "Correlation-based feature selection for machine learning," Ph.D. dissertation, The University of Waikato, 1999.